

PII: S0017-9310(96)00052-X

# The influence of radiation absorption on solar pond stability

M. GIESTAS†, H. PINA‡ and A. JOYCE†

†Departamento de Energias Renováveis, INETI, Estrada do Paço do Lumiar, 1699 Lisboa Cedex, Portugal

‡Instituto Superior Técnico, Portugal

(Received 22 September 1994 and in final form 18 January 1996)

**Abstract**—This paper presents a study of the gravitational stability of a salty layer of a fluid subject to an adverse temperature gradient as a result of heat absorption. This is intended to model solar ponds where an artificial gradient of salt concentration in water is used to prevent convective motions induced by the absorption of solar radiation. The stability of the Boussinesq approximation of the Navier–Stokes equations is analysed for perturbations of a certain kind imposed on the stationary solution. The marginal states for the onset of convection are obtained using a Galerkin method based on a weak formulation of the governing equations. The analysis considers solar energy absorption in the layer and assumes prescribed heat flux values as boundary conditions for the temperature equation. Results are compared with those obtained earlier by different authors for a layer of fluid, heated from below, with linear profiles of both salt concentration and temperature. Copyright © 1996 Elsevier Science Ltd.

## INTRODUCTION

A solar pond is a basin of water where a salinity gradient is artificially created in order to prevent the convection induced by the absorption of solar radiation. In a solar pond there are typically three well defined zones, as shown schematically in Fig. 1.

The surface and storage zones are convective zones where the temperature can be considered uniform, apart from interfacial boundary layers. In the gradient zone the salt gradient prevents convection and, as a result of solar energy absorption, a gradient of temperature is established. Water being a poor conductor of heat, the gradient zone functions as a transparent

insulation so that the heat absorbed is trapped and stored in the storage zone.

The gradient zone is thus a double diffusive layer of salt and temperature. Since the diffusivities of these two components are quite different, instabilities of the double diffusive type may occur (cf. Veronis [1]) and may lead to steady convective motions, therefore decreasing the insulation properties of the layer. The main problem of a solar pond is thus to maintain the nonconvectivity of the gradient zone and its stability.

Previous thermohaline convection studies have considered a layer with linear profiles for the temperature and salt concentration and imposed values for the boundary conditions relative to these variables,

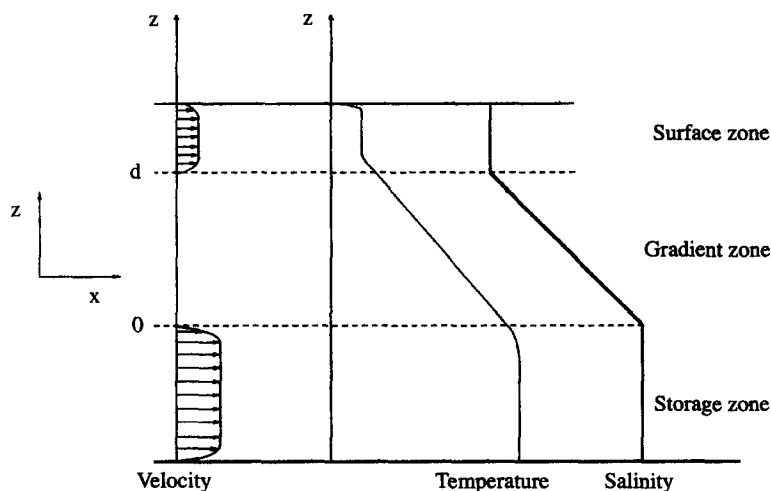


Fig. 1. Solar pond structure.

### NOMENCLATURE

<p><math>a</math> coefficient [derived from equation (17)]</p> <p><math>a_1(t), a_2(t), b_1(t), b_2(t), c_1(t)</math> coefficients, equations (68)–(72)</p> <p><math>A_1, A_2, B_1, B_2, C_1</math> constants</p> <p><math>d</math> depth of gradient zone [m]</p> <p><math>D_1, D_2, D_3</math> coefficients, equation (82)</p> <p><math>E, F</math> coefficients, equations (88), (89)</p> <p><math>g</math> acceleration of gravity [<math>m\ s^{-2}</math>]</p> <p><math>h_d</math> natural convection heat transfer coefficient [<math>W\ m^{-2}\ C^{-1}</math>]</p> <p><math>i</math> imaginary unit (<math>\sqrt{-1}</math>)</p> <p><math>\bar{k}</math> unit vector pointing upwards</p> <p><math>k_T, k_S</math> thermal and salt diffusivities [<math>m^2\ s^{-1}</math>]</p> <p><math>K_w</math> thermal conductivity of water [<math>W\ m^{-1}\ C^{-1}</math>]</p> <p><math>L</math> differential operator</p> <p><math>p</math> pressure [<math>N\ m^{-2}</math>]</p> <p><math>L_1, L_2, L_3, m_1, m_2</math> coefficients, equations (68)–(72)</p> <p><math>q(d)</math> heat flux at upper boundary (<math>z = d</math>) [<math>W\ m^{-2}</math>]</p> <p><math>\dot{q}</math> rate of energy generation per unit volume [<math>W\ m^{-3}</math>]</p> <p><math>q_{ext}</math> extracted heat flux in lower convective zone [<math>W\ m^{-2}</math>]</p> <p><math>q_{abs}</math> absorbed heat flux in lower convective zone [<math>W\ m^{-2}</math>]</p> <p><math>R_a, R_S</math> Rayleigh numbers for temperature and salinity</p> <p><math>s</math> eigenvalue, equation (82)</p> <p><math>S</math> salinity [<math>kg\ m^{-3}</math>]</p> <p><math>t</math> time [s]</p> <p><math>T</math> temperature [<math>^{\circ}C</math>]</p> <p><math>T(d)</math> temperature value at top boundary [<math>^{\circ}C</math>]</p>	<p><math>T_c</math> upper convective zone temperature [<math>^{\circ}C</math>]</p> <p><math>u, v, w</math> velocity components [<math>m\ s^{-1}</math>]</p> <p><math>\mathbf{v}</math> velocity field</p> <p><math>x, y, z</math> Cartesian co-ordinates.</p> <p><b>Greek symbols</b></p> <p><math>\alpha</math> coefficient of thermal expansion [<math>C^{-1}</math>]</p> <p><math>\beta</math> coefficient of salt expansion [<math>m^3\ kg^{-1}</math>]</p> <p><math>\lambda</math> cell typical length in the <math>x</math> direction [m]</p> <p><math>\rho, \rho_m</math> density and mean density [<math>kg\ m^{-3}</math>]</p> <p><math>\varphi_i, \zeta_i, \omega_i</math> trial functions</p> <p><math>\tau</math> inverse Schmidt number</p> <p><math>\psi</math> stream function</p> <p><math>\nu</math> kinematic viscosity [<math>m^2\ s^{-1}</math>]</p> <p><math>\mu</math> extinction coefficient [<math>m^{-1}</math>]</p> <p><math>\sigma_{xz}</math> shear stress [<math>N\ m^{-2}</math>]</p> <p><math>\omega_0</math> frequency of oscillation [<math>s^{-1}</math>].</p> <p><b>Superscripts</b></p> <p>(<math>x</math>) undisturbed variable</p> <p>(<math>\bar{x}</math>) perturbed variable</p> <p>(<math>\dot{x}</math>) a dimensional variable</p> <p>(<math>\dot{x}</math>) time derivative.</p> <p><b>Special symbols</b></p> <p><math>\Delta T = T(0) - T(d)</math> thermal difference</p> <p><math>\Delta S = S(0) - S(d)</math> saline difference.</p> <p><math>\nabla\mathbf{v} = \begin{pmatrix} \frac{\partial \mathbf{v}}{\partial x}, \frac{\partial \mathbf{v}}{\partial y}, \frac{\partial \mathbf{v}}{\partial z} \end{pmatrix}</math></p> <p><math>\nabla^2 = \frac{\partial^2}{\partial x^2} + \frac{\partial^2}{\partial y^2} + \frac{\partial^2}{\partial z^2}</math></p> <p><math>J(f, \mathbf{g}) = \frac{\partial f}{\partial x} \frac{\partial \mathbf{g}}{\partial z} - \frac{\partial f}{\partial z} \frac{\partial \mathbf{g}}{\partial x}</math>.</p>
---	--

Veronis [1, 2], Schechter *et al.* [3]. However solar ponds seldom show linear profiles of both salinity and temperature, and the prescription of boundary values relative to these variables may not be adequate. The objective of this paper is to present an analysis where a physically more realistic hypothesis regarding the temperature profile is made.

The modelling of the gradient layer is based on the Boussinesq approximation of the Navier–Stokes equations [2–5]

momentum equation

$$\frac{\partial \mathbf{v}}{\partial t} + (\mathbf{v} \cdot \nabla) \mathbf{v} = -\frac{1}{\rho_m} \nabla p + \mathbf{g}(\alpha T - \beta S) \bar{k} + \nu \nabla^2 \mathbf{v} \quad (1)$$

continuity equation

$$\nabla \cdot \mathbf{v} = 0 \quad (2)$$

heat diffusion

$$\frac{\partial T}{\partial t} + \mathbf{v} \cdot \nabla T = k_T \nabla^2 T + \frac{\dot{q}}{\rho C_p} \quad (3)$$

salt diffusion

$$\frac{\partial S}{\partial t} + \mathbf{v} \cdot \nabla S = k_S \nabla^2 S \quad (4)$$

state equation

$$\rho = \rho_m (1 - \alpha T + \beta S), \quad (5)$$

where

$$\alpha = -\frac{1}{\rho} \left( \frac{\partial \rho}{\partial T} \right) \quad \beta = \frac{1}{\rho} \left( \frac{\partial \rho}{\partial S} \right). \quad (6)$$

For the sake of notational simplicity,  $T$  denotes the

temperature differential measured relative to a reference temperature for which  $\rho$  assumes the value  $\rho_m$ .

As shown in Fig. 1, a Cartesian coordinate system  $(x, y, z)$  is employed,  $x$  and  $y$  being the horizontal axis and  $z$  the vertical axis pointing upwards. The solar pond is supposed infinite in the  $x$ - and  $y$ -directions. The analysis assumes a purely two-dimensional situation where all variables depend exclusively on the  $x$ - and  $z$ -coordinates and on the time  $t$ .

The steady-state solutions are obtained by making the velocity  $v$  and all time derivatives equal to zero in equations (1)–(5). The stability of the gradient layer will be studied by superposing perturbations upon these steady-state solutions.

In the present paper the time evolution of these perturbations is analysed by using a weak formulation of the governing equations and a Galerkin method to obtain approximate solutions. Therefore this procedure leads in the end to a nonlinear system of ordinary differential equations.

The study of the stability of the double diffusive layer, i.e. the conditions for which the layer remains nonconvective, is based on the linearization of this system of ordinary differential equations.

In order to gain some insight into the nonlinear dynamic behaviour of the double diffusive layer the nonlinear system of ordinary differential equations is solved by a numerical method and the results are represented in a properly chosen phase space.

### STEADY-STATE SOLUTION

The steady-state equation for salinity  $S_s(z)$  is obtained from equation (4) by setting the time derivative to zero

$$\frac{\partial^2 S_s}{\partial z^2} = 0. \tag{7}$$

The boundary conditions for this equation are obtained assuming that the storage zone is near saturation and that salinity is kept low at the surface zone. These two zones can be considered as having infinite capacity allowing therefore the values of salinity at the boundaries of the gradient zone to be imposed, i.e.

$$S_s|_{z=0} = S_0 \tag{8a}$$

$$S_s|_{z=d} = S_1. \tag{8b}$$

Under these assumptions the steady solution of the salt diffusion equation (4) is simply

$$S_s(z) = \frac{S_1 - S_0}{d} z + S_0. \tag{9}$$

The steady-state solution  $T_s(z)$  for the temperature is determined considering that the absorption of solar radiation can be modelled by an extinction coefficient  $\mu$  that takes into account the transparency of the fluid

(Lambert law). The rate of energy generation per unit volume in the layer can thus be expressed by

$$\dot{q}(z) = q(d)\mu \exp(-\mu(d-z)) \tag{10}$$

where  $q(d)$  is the heat flux due to solar radiation at the upper boundary of the gradient zone, ( $z = d$ ). Under these hypotheses the steady-state heat diffusion equation (3) in a layer with heat generation becomes

$$\frac{\partial^2 T_s}{\partial z^2} = -\frac{\dot{q}(z)}{K_w}. \tag{11}$$

At both boundaries of the gradient zone, the heat flux is prescribed as follows:

$$\left. \frac{\partial T_s}{\partial z} \right|_{z=0} = -\frac{q}{K_w} \tag{12a}$$

$$\left. \frac{\partial T_s}{\partial z} \right|_{z=d} = -\frac{h_d(T_s(d) - T_\infty)}{K_w}. \tag{12b}$$

For the top boundary, equation (12b), the heat flux from the gradient zone must be equal to the heat transferred to the surface zone by convection. In this equation  $T_s(d)$  is the temperature at the top boundary,  $T_\infty$  is the surface zone temperature (Fig. 1),  $h_d$  is the convective heat transfer coefficient and  $K_w$  is the thermal conductivity of the water. For the lower boundary, equation (12a), the heat flux  $-K_w(\partial T_s/\partial z)$  is equal to the heat flux  $q$  coming from the storage zone.

Since the bottom of the pond is considered to be perfectly insulated, the heat flux from the storage zone must be equal to the difference between the total heat absorbed in the storage zone per unit area  $q_{abs}$  and the total heat extracted per unit area in the same zone  $q_{ext}$

$$q = q_{abs} - q_{ext} \tag{13}$$

thereby guaranteeing a global energy balance.

Given the asymptotic behaviour of the radiation absorption in the pond and in order to simplify the resulting expression, we assume for the calculation of the total heat absorbed in the storage zone  $q_{abs}$  an infinite height of the lower convective zone, and so

$$q_{abs} = \int_{-\infty}^0 \dot{q}(z) dz = q(d) \exp(-\mu d). \tag{14}$$

The heat flux extracted can be conveniently represented as a fraction  $f$  of the total heat flux absorbed in the bottom convective zone and thus, it may be written according to

$$q = q_{abs} - q_{ext} = (1-f)q_{abs} = (1-f)q(d) \exp(-\mu d). \tag{15}$$

The steady-state temperature profile  $T_s(z)$  is easily obtained solving equation (11) with boundary conditions (12a) and (12b), leading to

Table 1.

$T_s = 20^\circ\text{C}$
$K_w = 0.6 \text{ W m}^{-1} \text{ }^\circ\text{C}^{-1}$
$h_d = 100 \text{ W m}^{-2} \text{ }^\circ\text{C}^{-1}$
$q(d) = \begin{cases} 50 \text{ W m}^{-2} & \text{for } \mu = 0.2 \\ 66 \text{ W m}^{-2} & \text{for } \mu = 0.8 \end{cases}$

$$T_s(z) = T_s + \frac{q(d)}{K_w} \exp(-\mu d) \times \left[ -\frac{\exp(\mu z)}{\mu} + f(z-d) \right] - \frac{f}{h_d} (q(d) \exp(-\mu d)) + q(d) \left[ \frac{1}{h_d} + \frac{1}{K_w \mu} \right]. \quad (16)$$

The steady-state salt and temperature solutions, equations (9) and (16) for the case of zero energy extracted at the bottom ( $f = 0$ ) and the typical values shown in Table 1, are presented in Fig. 2.

These profiles seem to yield a more realistic representation of the experimental data obtained in solar ponds [6–8], as compared with the linear profiles used in previous analysis.

The worst situation for the onset of instabilities occurs when there is no heat extraction from the pond, i.e. when  $f = 0$ , and thus with a stronger temperature gradient. In this case equation (16) turns to

$$T_s(z) = T_s - a \left[ \frac{\exp(\mu z)}{\mu} \right] + q(d) \left[ \frac{1}{h_d} + \frac{1}{K_w \mu} \right], \quad (17)$$

where

$$a = \frac{q(d)}{K_w} \exp(-\mu d). \quad (18)$$

**LINEAR DYNAMIC STABILITY ANALYSIS**

The downward increase of the fluid density  $\rho$  in the gradient layer is not sufficient to guarantee its stability. In fact, double-diffusive phenomena can lead to insta-

bilities even when  $\partial\rho/\partial z < 0$  as shown by Turner [9], thus making a dynamic analysis unavoidable.

To conduct this analysis two approaches are possible: to solve approximately the governing equations (1)–(5) using, for example, a Fourier type expansion for the dependent variables as in refs. [1, 3, 4] or to cast those equations into a weak form followed by a Galerkin type approximation [10, 11]. As this later procedure was more amenable to the introduction of natural boundary conditions it was chosen for the present study.

*Problem formulation*

The continuity equation (2) can be identically satisfied by introducing the stream function  $\psi$  defined by

$$\mathbf{v} = (u, v, w) = \left( \frac{\partial\psi}{\partial z}, 0, -\frac{\partial\psi}{\partial x} \right) \quad (19)$$

as a dependent variable replacing the velocity  $\mathbf{v}$ .

The dependent variables  $\psi$ ,  $T$  and  $S$  are expressed as the sum of the steady-state and perturbation terms. Therefore,  $\psi$ ,  $T$  and  $S$  can be written as

$$\psi(x, z, t) = \psi_s(z) + \tilde{\psi}(x, z, t) \quad (20)$$

$$T(x, z, t) = T_s(z) + \tilde{T}(x, z, t) \quad (21)$$

$$S(x, z, t) = S_s(z) + \tilde{S}(x, z, t), \quad (22)$$

where  $(\tilde{\quad})$  denotes a perturbation term. The set of equations (1)–(5) then becomes

$$\left( \frac{1}{Pr} \frac{\partial}{\partial t} - \nu \nabla^2 \right) \nabla^2 \tilde{\psi} = \mathbf{g} \left( \alpha \frac{\partial \tilde{T}}{\partial x} - \beta \frac{\partial \tilde{S}}{\partial x} \right) + \frac{1}{Pr} J(\tilde{\psi}, \nabla^2 \tilde{\psi}) \quad (23)$$

$$\left( \frac{\partial}{\partial t} - k_T \nabla^2 \right) \tilde{T} = J(\tilde{\psi}, \tilde{T}) - \frac{\partial \tilde{\psi}}{\partial x} a [\exp(\mu z) - f] \quad (24)$$

$$\left( \frac{\partial}{\partial t} - k_S \nabla^2 \right) \tilde{S} + \frac{\partial \tilde{\psi}}{\partial x} = J(\tilde{\psi}, \tilde{S}). \quad (25)$$

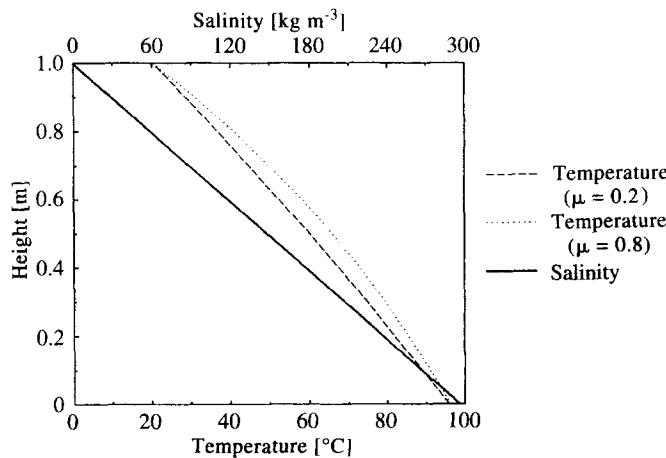


Fig. 2. Steady salt and temperature profiles ( $f = 0$ ).

The Jacobian  $J(\tilde{\psi}, \nabla^2 \tilde{\psi})$  in equation (23) results from the dot product  $\mathbf{v} \cdot \nabla \mathbf{v}$  from equation (1), where  $\mathbf{v}$  is expressed in terms of the stream function. In equation (24) the Jacobian  $J(\tilde{\psi}, \tilde{T})$  results from  $-\mathbf{v} \cdot \nabla T$  from equation (3) and in equation (25) the Jacobian  $J(\tilde{\psi}, \tilde{S})$  results from  $-\mathbf{v} \cdot \nabla S$  in equation (4). These Jacobians are the only nonlinear contributions to the right hand side of equations (23)–(25), and they reflect the effects of convection.

All the perturbations,  $\tilde{\psi}$ ,  $\tilde{T}$  and  $\tilde{S}$  are assumed to be periodic in  $x$  with period  $\lambda$ , implying that all motion takes place in a cell  $]0, \lambda[ \times ]0, d[$ .

It should be noted that since the steady state solutions were defined as corresponding to  $\mathbf{v} = \mathbf{0}$ ,  $\psi_s(z)$  is identically zero.

At the interfaces of the gradient zone it is assumed that no vertical motion takes place, i.e.

$$w|_{z=0} = 0, \quad w|_{z=d} = 0 \quad (26)$$

which are equivalent to :

$$\left. \frac{\partial \psi}{\partial x} \right|_{z=0} = 0, \quad \left. \frac{\partial \psi}{\partial x} \right|_{z=d} = 0. \quad (27)$$

Moreover, as a simplifying hypothesis usually made in double diffusive problems, shear free boundaries are assumed at the interfaces. Since shear stress is given by

$$\sigma_{xz} = \mu \left( \frac{\partial w}{\partial x} + \frac{\partial u}{\partial z} \right) \quad (28)$$

replacing the components of velocity in terms of stream function components yields

$$\sigma_{xz} = \mu \left( -\frac{\partial^2 \psi}{\partial x^2} + \frac{\partial^2 \psi}{\partial z^2} \right). \quad (29)$$

Introducing conditions (26) and (27), equation (29) gives the boundary conditions

$$\sigma_{xz}|_{z=0} = 0 \Rightarrow \left. \frac{\partial^2 \psi}{\partial z^2} \right|_{z=0} = 0 \quad (30a)$$

$$\sigma_{xz}|_{z=d} = 0 \Rightarrow \left. \frac{\partial^2 \psi}{\partial z^2} \right|_{z=d} = 0. \quad (30b)$$

The stream function is defined within an additive constant and therefore  $\psi$  is set to zero at  $z = 0$ . Since

$$\psi(d) = \psi(0) + \int_0^d \frac{\partial \psi}{\partial z} dz = \psi(0) + \int_0^d u(x, z) dz = \psi(0) \quad (31)$$

by the mass conservation principle, it follows that :

$$\psi|_{z=0} = 0 \quad (32a)$$

$$\psi|_{z=d} = 0. \quad (32b)$$

Boundary conditions for  $S$  and  $T$  are

$$S|_{z=0} = S_s|_{z=0} + \tilde{S}|_{z=0} \quad (33a)$$

$$S|_{z=d} = S_s|_{z=d} + \tilde{S}|_{z=d} \quad (33b)$$

$$\left. \frac{\partial T}{\partial z} \right|_{z=0} = \left. \frac{\partial T_s}{\partial z} \right|_{z=0} + \left. \frac{\partial \tilde{T}}{\partial z} \right|_{z=0} \quad (34a)$$

$$\left. \frac{\partial T}{\partial z} \right|_{z=d} = \left. \frac{\partial T_s}{\partial z} \right|_{z=d} + \left. \frac{\partial \tilde{T}}{\partial z} \right|_{z=d}. \quad (34b)$$

From the boundary conditions stated for the steady states for both salinity and temperature, the following expressions result :

$$\tilde{S}|_{z=0} = 0 \quad (35a)$$

$$\tilde{S}|_{z=d} = 0 \quad (35b)$$

$$\left. \frac{\partial \tilde{T}}{\partial z} \right|_{z=0} = 0 \quad (36a)$$

$$\left. \frac{\partial \tilde{T}}{\partial z} \right|_{z=d} = -\frac{h_a \tilde{T}}{K_w}. \quad (36b)$$

The set of equations (23)–(25) involving the perturbed variables  $\tilde{\psi}$ ,  $\tilde{T}$  and  $\tilde{S}$  can be non-dimensionalized by introducing the following non-dimensional variables denoted by ( $\hat{\cdot}$ ) :

$$\mathbf{v} = \left( \frac{k_T}{d} \right) \hat{\mathbf{v}} \quad \tilde{\psi} = k_T \hat{\psi} \quad \tilde{T} = (\Delta T) \hat{T} \quad \tilde{S} = (\Delta S) \hat{S} \quad (37)$$

$$x = d\hat{x}, \quad y = d\hat{y}, \quad z = d\hat{z} \quad t = \left( \frac{d^2}{k_T} \right) \hat{t} \quad (38)$$

$$\nabla = \frac{1}{d} \hat{\nabla} \quad \nabla^2 = \frac{1}{d^2} \hat{\nabla}^2 \quad (39)$$

$$\mu = \frac{\hat{\mu}}{d} \quad a = \hat{a} \frac{\Delta T}{d} \quad (40)$$

$$\hat{p} = \frac{pd^2}{\rho_m \nu k_T} \quad \tau = \frac{k_s}{k_T}. \quad (41)$$

The following set of nondimensionalized equations is therefore obtained :

$$\left( \frac{1}{Pr} \frac{\partial}{\partial \hat{t}} - \hat{\nabla}^2 \right) \hat{\nabla}^2 \hat{\psi} = -R_a \frac{\partial \hat{T}}{\partial \hat{x}} + R_s \frac{\partial \hat{S}}{\partial \hat{x}} + \frac{1}{Pr} J(\hat{\psi}, \hat{\nabla}^2 \hat{\psi}) \quad (42)$$

$$\left( \frac{\partial}{\partial \hat{t}} - \hat{\nabla}^2 \right) \hat{T} = J(\hat{\psi}, \hat{T}) - \frac{\partial \hat{\psi}}{\partial \hat{x}} a [\exp(\hat{\mu} \hat{z}) - f] \quad (43)$$

$$\left( \frac{\partial}{\partial \hat{t}} - \tau \hat{\nabla}^2 \right) \hat{S} + \frac{\partial \hat{\psi}}{\partial \hat{x}} = J(\hat{\psi}, \hat{S}), \quad (44)$$

where

$$R_a = \frac{g\alpha\Delta T d^3}{k_{Tv}}; \quad R_s = \frac{g\beta\Delta S d^3}{k_{Tv}} \quad (45)$$

are, respectively, the thermal Rayleigh number and the salinity Rayleigh number.

From equations (32)–(34) the following boundary conditions are derived for the nondimensional equations (42)–(44):

$$\frac{\partial^2 \hat{\psi}}{\partial \hat{z}^2} \Big|_{\hat{z}=0} = \frac{\partial^2 \hat{\psi}}{\partial \hat{z}^2} \Big|_{\hat{z}=1} = 0 \tag{46a}$$

$$\hat{\psi} \Big|_{\hat{z}=0} = \hat{\psi} \Big|_{\hat{z}=1} = 0 \tag{46b}$$

$$\frac{\partial^2 \hat{\psi}}{\partial \hat{x}^2} \Big|_{\hat{x}=0} = \frac{\partial^2 \hat{\psi}}{\partial \hat{x}^2} \Big|_{\hat{x}=\lambda} = 0 \tag{46c}$$

$$\hat{\psi} \Big|_{\hat{x}=0} = \hat{\psi} \Big|_{\hat{x}=\lambda} = 0 \tag{46d}$$

$$\hat{S} \Big|_{\hat{z}=0} = \hat{S} \Big|_{\hat{z}=1} = 0 \tag{47a}$$

$$\frac{\partial \hat{S}}{\partial \hat{x}} \Big|_{\hat{x}=0} = \frac{\partial \hat{S}}{\partial \hat{x}} \Big|_{\hat{x}=\lambda} = 0 \tag{47b}$$

$$\frac{\partial \hat{T}}{\partial \hat{z}} \Big|_{\hat{z}=0} = 0 \tag{48a}$$

$$\frac{\partial \hat{T}}{\partial \hat{z}} \Big|_{\hat{z}=1} = -\frac{h_0 d}{K_w} \hat{T} \tag{48b}$$

$$\frac{\partial \hat{T}}{\partial \hat{x}} \Big|_{\hat{x}=0} = \frac{\partial \hat{T}}{\partial \hat{x}} \Big|_{\hat{x}=\lambda} = 0. \tag{48c}$$

The sign (^) denoting nondimensional variables will be dropped with the understanding that from now on all variables are nondimensional.

*Approximate formulation*

The problem (42)–(44) will be recast into a weak formulation similar to those used in Finlayson [10] and Magen *et al.* [11].

For the sake of brevity the salinity equation will be employed to illustrate the procedure adopted, the case for the remaining equations offering no additional difficulties.

Equation (44) will be written in the form

$$LS = f, \tag{49}$$

where  $L$  denotes the differential operator defined by

$$L(\cdot) = \left( \frac{\partial}{\partial t} - \tau \nabla^2 \right) (\cdot) - J(\psi, \cdot). \tag{50}$$

$S$  is considered to be approximated by the following linear combination:

$$S(x, z, t) \cong S_n(x, z, t) = \sum_{i=1}^n b_i(t) \varphi_i(x, z), \tag{51}$$

where the  $\varphi_i$ s are linearly independent functions generating the subspace  $\mathcal{T}_n$  of trial functions. Note that equation (51) clearly decouples the time and spatial dependencies. The residual of equation (50) is given by

$$r = LS_n - f = L\left(\sum_{i=1}^n b_i \varphi_i\right) - f. \tag{52}$$

To obtain the coefficients  $b_i$ ,  $r$  is required to be orthogonal to the subspace  $\mathcal{T}_n$  of trial functions, i.e.

$$\int_{\Omega} r \varphi \, dx \, dz = 0 \quad \forall \varphi \in \mathcal{T}_n. \tag{53}$$

Since  $\varphi_j$  forms a basis of  $\mathcal{T}_n$  this is equivalent to the following system of equations.

$$\int_{\Omega} r \varphi_j \, dx \, dz = 0, \quad j = 1, \dots, n \tag{54}$$

or

$$\sum_{i=1}^n \int_{\Omega} L(b_i \varphi_i) \varphi_j \, dx \, dz = \int_{\Omega} f \varphi_j \, dx \, dz, \quad j = 1, \dots, n. \tag{55}$$

The usual integration by parts is invoked to reduce the order of the derivatives present in the left hand side of equation (55), and at the same time incorporate the natural boundary conditions if necessary. Starting from equations (44), the following expression is obtained:

$$\int_{\Omega} \left( \frac{\partial S_n}{\partial t} - \tau \nabla^2 S_n + \frac{\partial \psi_n}{\partial x} - J(\psi_n, S_n) \right) \varphi_j \, d\Omega = 0 \tag{56a}$$

or

$$\int_{\Omega} \frac{\partial S_n}{\partial t} \varphi_j \, d\Omega + \int_{\Omega} \frac{\partial \psi_n}{\partial x} \varphi_j \, d\Omega - \int_{\Omega} J(\psi_n, S_n) \varphi_j \, d\Omega - \tau \int_{\Omega} (\nabla^2 S_n) \varphi_j \, d\Omega = 0. \tag{56b}$$

An integration by parts in the last term leads to

$$\int_{\Omega} (\nabla^2 S_n) \varphi_j \, d\Omega = \int_{\Omega} \nabla(\nabla S_n) \varphi_j \, d\Omega \tag{57a}$$

or

$$\int_{\Omega} (\nabla^2 S_n) \varphi_j \, d\Omega = \int_{\Gamma} (\nabla S_n \cdot n) \varphi_j \, d\Gamma - \int_{\Omega} \nabla S_n \cdot \nabla \varphi_j \, d\Omega, \tag{57b}$$

where  $\Gamma$  denotes the boundary of  $\Omega$ .

The boundary conditions (47) imply that the integrals over the boundaries  $\Gamma$  are zero, and since  $\varphi$  must satisfy the essential homogeneous boundary condition, expression (57) turns to

$$\int_{\Omega} (\nabla^2 S_n) \varphi_j \, d\Omega = - \int_{\Omega} \nabla S_n \cdot \nabla \varphi_j \, d\Omega. \tag{58}$$

Thereby equation (56b) becomes

$$\int_{\Omega} \frac{\partial S_n}{\partial t} \varphi_j \, d\Omega + \tau \int_{\Omega} \nabla S_n \cdot \nabla \varphi_j \, d\Omega + \int_{\Omega} \frac{\partial \psi_n}{\partial x} \varphi_j \, d\Omega - \int_{\Omega} J(\psi_n, S_n) \varphi_j \, d\Omega = 0. \quad (59)$$

By an analogous procedure, the weak formulation for  $T$  obtained from equation (43) is

$$\int_{\Omega} \frac{\partial T_n}{\partial t} \xi_j \, d\Omega + \int_{\Omega} \nabla T_n \nabla \xi_j \, d\Omega - \int_{\Omega} J(\psi_n, T_n) \xi_j \, d\Omega + \int_{\Omega} \frac{\partial \psi_n}{\partial x} a[\exp(\mu z) - f] \xi_j \, d\Omega = 0 \quad (60)$$

and from equation (42) the weak formulation for  $\psi$  is

$$\int_{\Omega} \frac{1}{Pr} \frac{\partial}{\partial t} (-\nabla \psi_n \cdot \nabla \omega_j) \, d\Omega - \int_{\Omega} \Delta \psi_n \Delta \omega_j \, d\Omega + \int_{\Omega} \left( R_a \frac{\partial T_n}{\partial x} - R_s \frac{\partial S_n}{\partial x} \right) \omega_j \, d\Omega - \frac{1}{Pr} \int_{\Omega} J(\psi_n, \nabla^2 \psi_n) \omega_j \, d\Omega = 0. \quad (61)$$

The framework presented above allows for an arbitrary value of  $n$ . The choice of the actual value is dictated by the need on one hand to represent the physics of the problem at least within engineering accuracy and on the other hand to keep the computational complexity at a reasonable level.

The value  $n = 2$  was adopted in the present study. Greater values of  $n$  were tried leading to a negligible improvement, but at the cost of an exaggerated increase in complexity. The trial functions for  $S$ ,  $T$  and  $\psi$  considered are

$$S_2 = b_1(t) \varphi_1(x, z) + b_2(t) \varphi_2(x, z) \quad (62)$$

with

$$\varphi_1(x, z) = z(1-z); \quad \varphi_2(x, z) = z(1-z) \cos\left(\frac{2\pi x}{\lambda}\right) \quad (63)$$

$$T_2 = a_1(t) \xi_1(x, z) + a_2(t) \xi_2(x, z) \quad (64)$$

with

$$\xi_1(x, z) = \varphi_1(x, z) \quad \text{and} \quad \xi_2(x, z) = \varphi_2(x, z) \quad (65)$$

$$\psi_1 = c_1(t) \omega_1(x, z) \quad (66)$$

where

$$\omega_1(x, z) = z^2(1-z) \sin\left(\frac{2\pi x}{\lambda}\right). \quad (67)$$

Experiments revealed that the results were not overly sensitive to the choice of trial functions pro-

vided that the underlying essential physical features were well modelled.

For  $S$ , the choice of the basis functions for the subspace  $\mathcal{F}_n$  was dictated by the following reasons: the need to satisfy the essential boundary conditions, i.e. equations (47), to satisfy the periodicity in  $x$  and to retain only terms up to the second degree in  $z$ .

For simplicity, and according to equations (48), the trial functions for  $T$  were chosen to be similar to  $S$ . The trial function proposed for  $\psi$  verifies the essential boundary conditions (46b) and (46d). Boundary conditions (46a) and (46c) need not be satisfied in a weak formulation context.

After substituting (62) and (63) into equation (59), two ordinary differential equations for the time dependent coefficients  $b_1(t)$  and  $b_2(t)$  are obtained, the details are given below. Substituting equations (64) and (65) into equation (60), two ordinary differential equations for the time dependent coefficients  $a_1(t)$  and  $a_2(t)$  are also obtained. Finally, after substituting equations (66) and (67) into equation (61) an ordinary differential equation for the time dependent coefficient  $c_1(t)$  is obtained.

Collecting these results, the following system of ordinary differential equations for the coefficients  $a_1(t)$ ,  $a_2(t)$ ,  $b_1(t)$ ,  $b_2(t)$ ,  $c_1(t)$  is obtained

$$\dot{a}_1 = -10a_1 + \frac{\pi}{14\lambda} c_1 a_2 \quad (68)$$

$$\dot{a}_2 = -\frac{2}{\lambda} L_2 a_2 - \frac{\pi}{\lambda} \left[ a(m_1 + 60m_2 - f) + \frac{1}{7} a_1 \right] c_1 \quad (69)$$

$$\dot{b}_1 = -10\tau b_1 + \frac{\pi}{14\lambda} c_1 b_2 \quad (70)$$

$$\dot{b}_2 = -\frac{2}{\lambda} \tau L_2 b_2 - \frac{\pi}{\lambda} \left( 1 + \frac{1}{7} b_1 \right) c_1 \quad (71)$$

$$\dot{c}_1 = -2PrL_1 L_3 c_1 - \frac{7}{4} PrL_1 \pi \lambda (R_a a_2 - R_s b_2), \quad (72)$$

where

$$L_1 = \frac{1}{(7\lambda^2 + 2\pi^2)} \quad L_2 = \frac{5\lambda^2 + 2\pi^2}{\lambda} \quad L_3 = \frac{105\lambda^4 + 28\lambda^2 \pi^2 + 4\pi^4}{\lambda^2} \quad (73)$$

$$m_1 = \frac{120 \exp(\mu) [\mu^3 - 9\mu^2 + 36\mu - 60]}{\mu^6}$$

$$m_2 = \frac{6(\mu^2 + 8\mu + 20)}{\mu^6}. \quad (74)$$

Within the validity of the approximations made, the solar pond stability is therefore reduced to the

study of the stability of the above system of ordinary differential equations.

*The marginal states*

Equations (68)–(72) form a nonlinear system of ordinary differential equations whose stability is difficult to assess. As usual in such circumstances the present analysis proceeds by linearization about the origin (the steady state), therefore neglecting all second-order terms.

The following linear system of ordinary differential equations is thus obtained:

$$\dot{a}_1 = -10a_1 \tag{75}$$

$$\dot{a}_2 = -\frac{2}{\lambda}L_2a_2 - \frac{\pi}{\lambda}[a(m_1 + 60m_2 - f)]c_1 \tag{76}$$

$$\dot{b}_1 = -10\tau b_1 \tag{77}$$

$$\dot{b}_2 = -\frac{2}{\lambda}\tau L_2b_2 - \frac{\pi}{\lambda}c_1 \tag{78}$$

$$\dot{c}_1 = -2PrL_1L_3c_1 - \frac{7}{4}PrL_1\pi\lambda(R_4a_2 - R_5b_2). \tag{79}$$

Solutions for these sets of equations of the form

$$\begin{cases} a_1(t) = A_1 \exp(st) \\ a_2(t) = A_2 \exp(st) \\ b_1(t) = B_1 \exp(st) \\ b_2(t) = B_2 \exp(st) \\ c_1(t) = C_1 \exp(st) \end{cases} \tag{80}$$

are searched for, where  $s$  is a complex number and the  $A_s$ ,  $B_s$  and  $C_s$  are constant amplitudes. Substituting these relations into equations (75)–(79), the following homogeneous system of algebraic equations is obtained:

$$\begin{bmatrix} 2PrL_1L_3 + s & 0 & \frac{7}{4}PrL_1\pi\lambda R_4 & 0 & -\frac{7}{4}PrL_1\pi\lambda R_5 \\ 0 & 10 + s & 0 & 0 & 0 \\ \frac{\pi}{\lambda}A & 0 & \frac{2}{\lambda}L_2 + s & 0 & 0 \\ 0 & 0 & 0 & 10\tau + s & 0 \\ \frac{\pi}{\lambda} & 0 & 0 & 0 & \frac{2}{\lambda}\tau L_2 + s \end{bmatrix} \begin{bmatrix} C_1 \\ A_1 \\ A_2 \\ B_1 \\ B_2 \end{bmatrix} = \begin{bmatrix} 0 \\ 0 \\ 0 \\ 0 \\ 0 \end{bmatrix}, \tag{81}$$

where  $A = a(m_1 + 60m_2 - f)$ .

For this system to have nontrivial solutions it is necessary that  $\det(\mathbf{M}) = 0$ ,  $\mathbf{M}$  being the matrix of system (81). This relation yields a fifth-degree polynomial equation in  $s$ , which may be written as

$$p_5(s) = (s + 10)(s + 10\tau)p_3(s) \tag{82}$$

with

$$p_3(s) = s^3 + D_1s^2 + D_2s + D_3, \tag{83}$$

where

$$D_1 = \frac{2L_2}{\lambda}(\tau + 1) + 2PrL_1L_3 \tag{84}$$

$$D_2 = \frac{4L_2}{\lambda} \left( \frac{L_2}{\lambda} \tau + (\tau + 1)PrL_1L_3 \right) + \frac{7\pi^2}{4}PrL_1(R_5 - AR_4) \tag{85}$$

$$D_3 = \frac{8\tau PrL_1L_2^2L_3}{\lambda^2} + \frac{7\pi^2}{2\lambda}PrL_1L_2(R_5 - A\tau R_4). \tag{86}$$

Since  $s = -10$  and  $s = -10\tau$  are negative zeros of the polynomial  $p_5(s)$ , the stability of system (80) depends on the nature of the roots of the third-degree polynomial  $p_3(s)$  in equation (82). The following cases must be distinguished according to the nature of the real part,  $Re(s)$ , of  $s$ :

- (a)  $Re(s) < 0$ , corresponds to an exponential decay of the perturbations: the steady state is asymptotically stable;
- (b)  $Re(s) > 0$ , corresponds to an exponential growth of the perturbations leading to unbounded linear instability, with no physical meaning;
- (c)  $Re(s) = 0$ . Two situations must be considered:  $s \neq 0$  and  $s = 0$ .

*Case*  $Re(s) = 0, s \neq 0$ . For  $s \neq 0$  one can write  $s = i\omega_0$ , where  $\omega_0$  is a real number and represents the angular frequency of the perturbation, corresponding to the onset of periodic motions sometimes referred to as overstability. Substituting  $s = i\omega_0$  in the third-

degree polynomial  $p_3(s)$  of equation (83), two equations are found: one for the real part and another for the imaginary part. The second yields an expression for  $\omega_0^2$ , which when substituted in the first produces the equation corresponding to the marginal state for



the onset of oscillatory motions, resulting in the following expression for the marginal states :

$$R_a = E \left( \frac{Pr + \tau F}{Pr + F} \right) R_s + \frac{16}{7} E \frac{(1 + \tau) L_2 (Pr + \tau F)}{Pr \pi^2 \lambda^2 L_1}, \quad (87)$$

where

$$E = f(\mu) = \frac{1}{A} \quad (88)$$

and

$$F = f(\lambda) = \frac{(5\lambda^2 + 2\pi^2)(7\lambda^2 + 2\pi^2)}{105\lambda^4 + 28\pi^2\lambda^2 + 4\pi^4}. \quad (89)$$

The frequency of oscillation  $\omega_0$  is given by

$$\omega_0^2 = \frac{4L_2}{\lambda} \left( \frac{L_2\tau}{\lambda} + PrL_1L_3(1 + \tau) \right) + \frac{7}{4} PrL_1\pi^2(R_s - AR_a). \quad (90)$$

Case  $Re(s) = 0, s = 0$ . Substituting  $s = 0$  in equation (82)  $D_3 = 0$  is obtained and from equation (86) it follows that :

$$R_a = E \frac{1}{\tau} R_s + \frac{16}{7} E \frac{L_2 L_3}{\pi^2 \lambda}. \quad (91)$$

Note that when  $s = 0$  the functions  $a_1(t), a_2(t), b_1(t), b_2(t)$  and  $c_1(t)$  are constant. This means that the convective motion has constant amplitude (independent of time), i.e. steady convective motion.

It may be noted that in equations (87), (90) and (91) the influence of the radiation absorption in the layer is conveyed by the parameter  $E$ , which depends exclusively on the value of the extinction coefficient  $\mu$ .

It can be easily verified that for large  $R_s$  values, as is usually the case for solar ponds ( $R_s$  of the order of  $10^9$ ), the second terms on the right hand sides of equations (87) and (91) are much smaller than the first terms, and therefore can be neglected. This leads to the relation

$$R_a = E \frac{Pr + \tau F}{Pr + F} R_s \quad (92)$$

and

$$R_a = E \frac{1}{\tau} R_s, \quad (93)$$

which are both similar to the results earlier obtained by Veronis [1]

$$R_a = \frac{Pr + \tau}{Pr + 1} R_s \quad (94)$$

and

$$R_a = \frac{1}{\tau} R_s. \quad (95)$$

Note that for oscillatory motion to occur the value of  $\omega_0$  must be real, which is equivalent to saying that  $\omega_0^2 > 0$ . Thus, the region where oscillatory motions can take place is defined by

$$R_a > E \left( \frac{Pr + \tau F}{Pr + F} \right) R_s + \frac{16}{7} E \frac{(1 + \tau) L_2 (Pr + \tau F)}{\pi^2 Pr L_1 \lambda^2} \quad (96)$$

and

$$R_a < ER_s + \frac{16}{7} E \frac{L_2 [L_2 \tau + Pr L_1 L_3 \lambda (1 + \tau)]}{\pi^2 Pr L_1 \lambda^2} \quad (97)$$

this last inequality resulting from the imposition of condition  $\omega_0^2 > 0$  in equation (90).

The value of  $\lambda$  that minimizes the right hand side of inequality (97) corresponds with the worst case for oscillatory motion to take place. To obtain this value, and for the sake of definiteness and exemplification, the following typical values for solar ponds are employed :

$$Pr = 7; \quad \tau = 0.01.$$

This leads to a value of  $\lambda$

$$\lambda = 2.1298.$$

Note that the nondimensional  $\lambda$  can be interpreted as the aspect ratio of the cells of the oscillatory motion. This value will be retained for the remainder of this study.

For the minimum value of  $\lambda$  mentioned above, the marginal states corresponding to equations (87) and (91) are therefore

$$R_a = 0.9249ER_s + 52.93E \quad (98)$$

$$R_a = 100ER_s + 1827.0E. \quad (99)$$

Increasing the dimension of the subspace of trial functions, within the constraints imposed by the physical problem, leads to a large increase of the algebraic complexity with no significant change on the final result. As an example for a subspace of dimension three the value of  $\lambda$  obtained was  $\lambda = 2.2925$  as compared with the previous value of  $\lambda = 2.1298$  obtained for a subspace of dimension two.

### RADIATION ABSORPTION CONTRIBUTION FOR THE MARGINAL STATES

Solar pond transparency has been studied for a long time. Rabl and Nielsen [12] proposed a sum of four exponentials, each one with its own extinction coefficient corresponding to the division of the solar spectrum in four wavelength intervals. In fact, the extinction coefficients proposed by these authors were obtained by measurements made on pure water and not on a real pond water which is generally affected by dust, debris and dissolved salts that decrease transparency. As stated before, the present study considers the absorption of radiation in the pond to have an exponential decay of the form

$$q(z) = q(d) \exp(-\mu(d-z)) \quad (100)$$

based on a single extinction coefficient  $\mu$ . The values of  $\mu$  are obtained by a least squares fitting of equation (100) to the experimental values of radiation absorption in pure water and in samples obtained from an experimental solar pond [13, 14].

Pure water corresponds to the minimum radiation absorption, i.e. good transparency. The water from the experimental solar pond represents the situation of weak transparency corresponding to higher values of  $\mu$ . The values of  $\mu$  obtained by the fitting procedure for a pond with an upper convective zone of 0.5 m and a gradient zone of 1 m are, respectively, for pure water  $\mu = 0.2$  and for the experimental solar pond  $\mu = 0.8$ .

As noted before the contribution of radiation absorption for the stability of the gradient zone is conveyed by the parameter  $E$  of equations (87) and (91) which depends exclusively on  $\mu$ .

It is clear that for low values of  $\mu$  the pond will develop greater gradients of temperature for the same value of the solar energy input. In this sense a good transparency pond will be more susceptible to instabilities than a poor transparency one.

However, in order to analyse the influence of radiation absorption in the stability of the gradient zone the comparison must be made for a situation where the same gradient of temperature is developed in the gradient zone, i.e. a situation where the value of  $R_a$  is the same for both profiles ( $\mu = 0.2$  and  $\mu = 0.8$ ). This situation is seen in Fig. 2 where the two steady-state temperature profiles were obtained for different solar energy inputs.

Figure 3 presents the marginal states for the onset of oscillatory motions, equation (87), for the two values of the extinction coefficient presented above, together with the marginal state obtained earlier by Veronis [1]. This figure was obtained considering the worst case for pond stability which, as mentioned before, occurs when no energy is extracted from the lower convective zone.

It can be seen that the marginal state for the onset of oscillatory motion for a poor transparency pond is below the corresponding marginal state for a good transparency pond, though the difference between the two curves decreases for high values of the salinity Rayleigh number  $R_s$  as generally found in solar ponds. This means that to maintain the nonconvectivity of the gradient zone for the same value of  $R_a$  one needs to have greater salinity gradients in poor transparency ponds.

Figure 3 also shows that the marginal states obtained in the present analysis are very close to the ones obtained earlier by Veronis [1], except the special cases of small values of  $R_a$  number, where the present analysis is more restrictive than the results obtained by Veronis [1]. The zone where periodic motions can occur is shown in Fig. 4 by the intersection of the half-planes defined by equations (96) and (97).

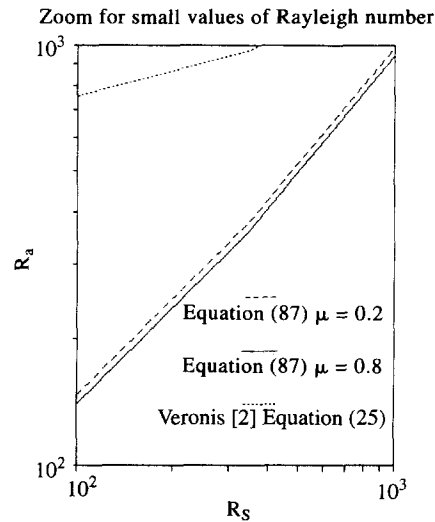
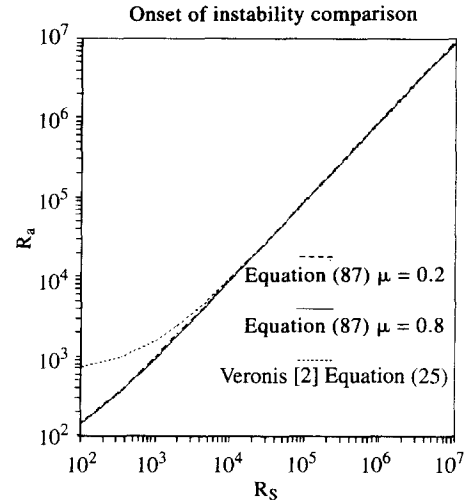


Fig. 3. Onset of instability comparison  $\mu = 0.8$ ,  $\mu = 0.2$   $\lambda = 2.1298$  and Veronis criteria.

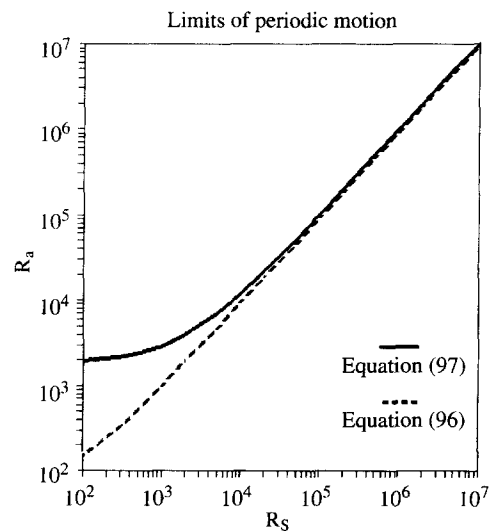


Fig. 4. Limits of periodic motion  $\mu = 0.8$ ;  $\lambda = 2.1298$ .

Figure 5 represents the marginal state for the onset of oscillatory motion [equation (87)], and the marginal state for steady convective motion [equation (91)] for  $\mu = 0.8$ . The instability proceeds through a periodic motion, from a region delimited by equation (87), until it reaches the steady convection motions whose marginal state is represented by equation (91).

**COMPARISON WITH PREVIOUS STUDIES**

Other authors Veronis [1, 2], Schechter *et al.* [3] and Turner [9], provided the basis for stability studies in double diffusion systems, namely thermohaline convection in solar ponds. In the absence of double diffusive problems, the criteria for stability of a gradient layer is obtained by setting  $\partial\rho/\partial z < 0$  and, taking in account the state equation (5), this leads to

$$R_s > R_a. \tag{101}$$

According to Veronis [1], a layer of fluid with both gradients of salt and temperature heated from below is maintained stable (nonconvective) if:

$$R_s > \frac{Pr+1}{Pr+\tau} R_a. \tag{102}$$

For the typical values of  $Pr$  and  $\tau$  mentioned above, one can obtain

$$R_s > 1.14R_a. \tag{103}$$

This means that, in order to keep the non-convectivity of the layer, the salinity gradient value must be at least 14% greater than the necessary value for the case where no double diffusive phenomena are present.

In the present study the results obtained for the same values of  $Pr$  and  $\tau$  are

$$R_s > 1.074R_a \text{ for } \mu = 0.2 \tag{104}$$

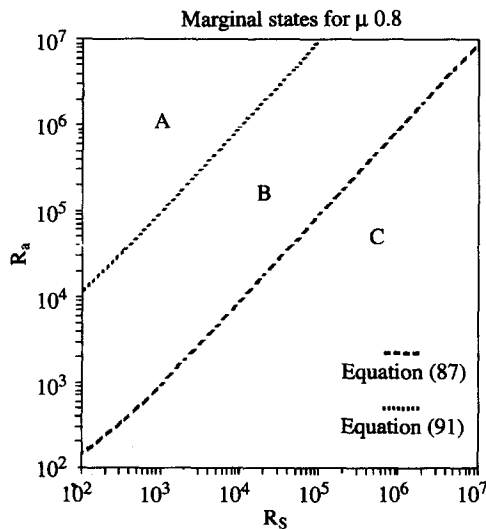


Fig. 5. Marginal states for stability  $\mu = 0.8$ ;  $\lambda = 2.1298$ .

$$R_s > 1.1257R_a \text{ for } \mu = 0.8. \tag{105}$$

In practical terms, the fact of having considered the absorption of radiation in the solar pond leads to the conclusion that less salt is required to maintain the nonconvectivity of the gradient layer, as compared with the amount of salt required by Veronis [1] analysis.

**NONLINEAR STABILITY ANALYSIS**

The linear stability analysis performed above required the neglecting of second-order terms. In order to verify that the results obtained are at least qualitatively independent of these approximations a numerical solution of the system of ordinary differential equations (68)–(72) was attempted.

This kind of study, which is in line with the work of Mukutmoni *et al.* [15, 16], requires the visualization of the dependent variables dynamic behaviour in an appropriate phase space. In the present work, the dynamic evolution of the nonlinear is depicted in a properly chosen phase space. The term that corresponds to velocity evolution with time is  $c_1(t)$ . For temperature, the product of both time coefficients  $a_1(t)$  and  $a_2(t)$  was chosen. The phase space  $(c_1(t), a_1(t) \cdot a_2(t))$  is chosen taking in account the fact that temperature is the leading variable of the process.

The system (68)–(72) of ordinary differential equations was solved by a fourth-order Runge–Kutta method with an adaptive step size control and Gill’s modification for roundoff errors compensation [17].

Some brief comments on the results obtained will be presented. Equations (87) and (91) are shown in Fig. 5 for  $\lambda = 2.1298$ ,  $\mu = 0.8$  and  $f = 0$  and establish different zones in the  $(R_s, R_a)$  plane corresponding each to a particular type of motion. To each zone a capital letter was assigned.

For points  $(R_s, R_a)$  in Zone A, a sink was detected, meaning a stable point with a nonzero velocity. This zone contains steady convective motion states.

For points  $(R_s, R_a)$  in Zone B, instabilities are expected to occur which are in agreement with the existence of aperiodic motions, as shown in Fig. 6.

For points  $(R_s, R_a)$  in Zone C, the trajectories rapidly fall to a point in phase space  $(c_1(t), a_1(t) \cdot a_2(t))$  with zero velocity, corresponding to the steady-state solution. This is the pure conductive zone predicted by the linear analysis above.

**CONCLUSIONS**

The stability of the gradient zone of a solar pond was analysed taking in account solar radiation absorption in the gradient layer.

The gradient zone of a solar pond is typically a double diffusive layer and previous analyses of its stability have considered the situation of a layer with linear profiles of salinity and temperature with prescribed values for these variables at both boundaries.

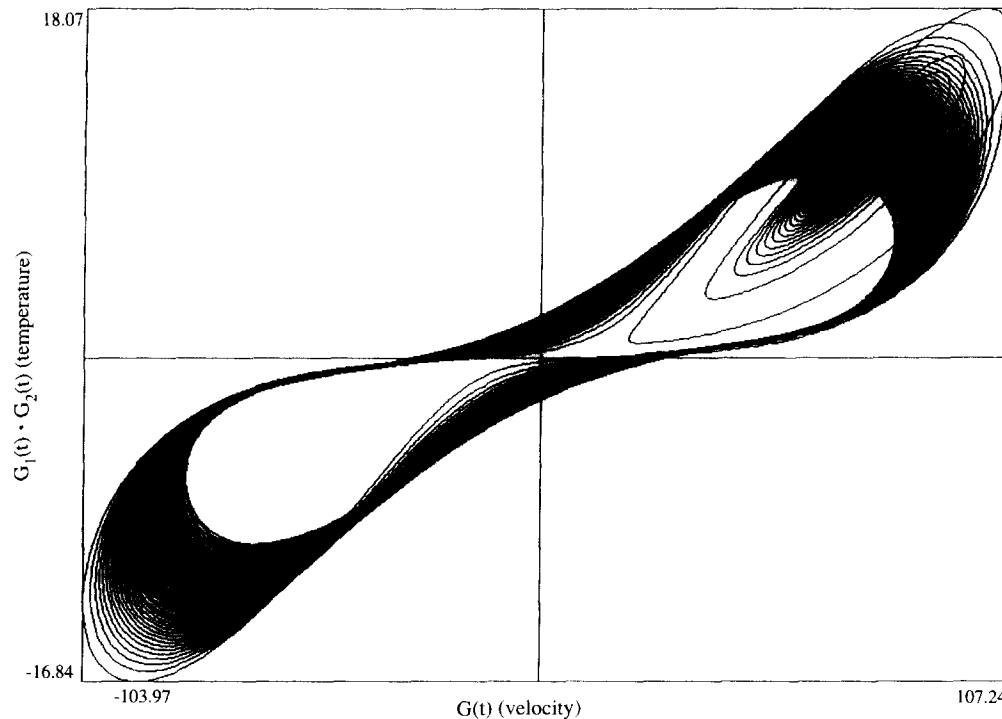


Fig. 6.  $c_1(t)$  vs  $a_1(t)a_2(t)$  in Zone B of  $(R_S, R_A)$  plane  $\mu = 0.8$ ;  $\lambda = 2.1298$ .

Nevertheless, in a solar pond, the absorption of solar radiation leads to nonlinear temperature profiles. These can only be obtained by considering absorption of solar radiation and by the imposition of flux boundary conditions.

The analysis of this problem, double diffusive layer with heat generation and flux boundary condition for temperature, is performed in this paper by solving the Boussinesq approximation of Navier–Stokes equations through a weak formulation of the equations and a Galerkin method. This method allows for a greater freedom of the boundary conditions as it is not too sensitive to the choice of the trial functions used, provided that they are realistic from a physical point of view.

The marginal states for the stability of the layer, in this case, show that a good transparency pond is less subjected to double diffusive instabilities when compared with a poor transparency pond with the same temperature gradient in the layer.

The results are in good agreement with the previous results obtained by Veronis [1] and others, though the consideration of heat generation in the layer showed that the marginal states are less restrictive, i.e. less salt is required to prevent convective motion.

In practical terms, this means that the fact of having considered the radiation absorption in the solar pond leads to the conclusion that less salt is required to maintain the nonconvectivity of the gradient layer. This requires, nevertheless, experimental evidence.

A brief nonlinear analysis was also performed in order to visualize in an appropriate space phase the

dynamics of the problem. The results were shown to be in agreement with those obtained from the linear analysis, leading to the conclusion that the trial functions need not be more complex than those that were selected.

*Acknowledgements*—The authors wish to thank INETI, Instituto Nacional de Engenharia e Tecnologia Industrial and IST, Instituto Superior Técnico for the computational facilities provided.

#### REFERENCES

1. G. Veronis, Effect of a stabilising gradient of solute on thermal convection, *J. Fluid Mech.* **34**, 315–336 (1968).
2. G. Veronis, On finite amplitude instability in thermohaline convection, *J. Mar. Res.* **23**, 1–17 (1964).
3. R. S. Schechter, M. G. Velarde and J. K. Platten, The two-component Bénard problem. In *Advances Chemical Physics* Vol. XXVI. Wiley, New York (1981).
4. L. N. Da Costa, E. Knobloch and N. O. Weiss, Oscillations in double-diffusive convection, *J. Fluid Mech.* **109**, 25–43 (1981).
5. D. A. Nield, D. M. Manole and J. L. Lage, Convection induced by inclined thermal and solute gradients in a shallow horizontal layer of a porous medium, *J. Fluid Mech.* **257**, 559–574 (1993).
6. J. R. Hull, Passive stabilisation of gradient zone boundaries in solar ponds, *Proceedings of the American Solar Energy Society*, Anaheim (1984).
7. F. Zangrando, On the hydrodynamics of salt-gradient solar ponds, *Solar Energy* **46**, 323–341 (1991).
8. A. Joyce, M. Giestas and H. Pina, The dynamics of free convection in a solar pond, *II World Renewable Energy Congress*, Reading, U.K. (1992).
9. J. S. Turner, Multicomponent convection, *A. Rev. Fluid Mech.* **17**, 11–14 (1985).

10. B. A. Finlayson, The Galerkin method applied to convective instability problems, *J. Fluid Mech.* **33**, 201–208 (1968).
11. M. Magen, D. Pnueli and Y. Zvirin, The stability chart of parallel shear flows with double diffusive processes—approximate derivation by a first-order Galerkin method, *Int. J. Heat Mass Transfer* **31**, 525–539 (1988).
12. A. Rabl and C. E. Nielsen, Solar ponds for space heating, *Solar Energy* **17**, 1–12 (1975).
13. A. A. Green, A. L. M. Joyce and M. Collares-Pereira, A spectrophotometric method for studying the transmission of radiation in a solar pond, *CEC Workshop on Optical Property Measurement Techniques*, Joint Research Centre ISPRA, Italy, 27–29 October (1987).
14. A. L. M. Joyce, Lagos solares; contribuição para o desenvolvimento de uma tecnologia, PhD thesis, University Nova de Lisboa, Faculdade Ciências e Tecnologia (1992).
15. D. Mukutmoni and K. T. Yang, Rayleigh–Bénard convection in a small aspect ratio enclosure; Part I—bifurcation to oscillatory convection, *J. Heat Transfer* **115**, 360–366 (1993).
16. D. Mukutmoni and K. T. Yang, Rayleigh–Bénard convection in a small aspect ratio enclosure; Part II—bifurcation to chaos, *J. Heat Transfer* **115**, 367–376 (1993).
17. A. Ralston and H. S. Will, *Mathematical Methods for Digital Computers*. Wiley, New York (1960).